Commun. Comput. Phys.
doi: 10.4208/cicp.2014.m400

Vol. **17**, No. 5, pp. 1169-1184
May 2015

Comparison of Simulations of Convective Flows

Pierre Lallemand[1] and François Dubois[2,3,*]

[1] *Beijing Computational Science Research Center, Beijing Run Ze Jia Ye, China.*
[2] *Structural Mechanics and Coupled Systems Laboratory, Conservatoire National des Arts et Métiers, Paris, France.*
[3] *Department of Mathematics, University Paris-Sud, Bât. 425, F-91405 Orsay Cedex, France.*

Received 23 December 2013; Accepted (in revised version) 27 June 2014

Abstract. We show that a single particle distribution for the "energy-conserving" D2Q13 lattice Boltzmann scheme can simulate coupled effects involving advection and diffusion of velocity and temperature. We consider various test cases: non-linear waves with periodic boundary conditions, a test case with buoyancy, propagation of transverse waves, Couette and Poiseuille flows. We test various boundary conditions and propose to mix bounce-back and anti-bounce-back numerical boundary conditions to take into account velocity and temperature Dirichlet conditions. We present also first results for the de Vahl Davis heated cavity. Our results are compared with the coupled D2Q9-D2Q5 lattice Boltzmann approach for the Boussinesq system and with an elementary finite differences solver for the compressible Navier-Stokes equations. Our main experimental result is the loss of symmetry in the de Vahl Davis cavity computed with the single D2Q13 lattice Boltzmann model without the Boussinesq hypothesis. This result is confirmed by a direct Navier Stokes simulation with finite differences.

AMS subject classifications: 6505, 76N15, 80A20, 82C20

Key words: Bounce-back, natural convection, adiabatic wall, de Vahl Davis.

1 Introduction

Lattice Boltzmann schemes have proven their efficiency for the computation of quasi-incompressible flows. We refer *e.g.* to [2, 9, 11] among others. In these cases, the physical conservations of mass and momentum are implemented in the framework of lattice Boltzmann schemes. When compressible effects are taken into account, it is necessary to

*Corresponding author. *Email addresses:* `pierre.lallemand1@free.fr` (P. Lallemand), `francois.dubois@math.u-psud.fr` (F. Dubois)

 ©2015 Global-Science Press

https://doi.org/10.4208/cicp.2014.m400 Published online by Cambridge University Press

add the conservation of energy. A classical approach is to begin with weakly compressible effects that can be modelled with the so-called Boussinesq approximation. In this case, the incompressibility condition remains a good approximation and coupled effects between conservations of momentum and energy are taken into account with a precise thermodynamical analysis. We refer to Landau [14] or Batchelor [1] for the derivation of the Boussinesq approximation. The implementation of the Boussinesq approximation is possible with the lattice Boltzmann approach with the introduction of two particle distributions. This idea has been also proposed in the context of finite volumes by the team of Perthame [10], and with lattice Boltzmann schemes by Eggels and Somers [5], Mezrhab *et al.* [16] and Wang *et al.* [21] among others.

In this contribution, we study a direct approximation of the compressible Navier Stokes equations with an "energy-conserving" lattice Boltzmann scheme using a single particle distribution. A first tentative study [12] has shown that for a critical value of the Prandlt number, the thermal wave and the viscous one merge together, the physics is badly represented and an instability occurs in general. In consequence, no satisfying compressible flows have been obtained with this direct numerical modelling. In a second tentative [13], we have analyzed with great details several lattice Boltzmann schemes with four conservation laws in two space dimensions. With an adequate fitting of the parameters of the scheme, it is possible to enlarge the zone in the spectral space where the thermal and viscous waves remain decoupled. Moreover, these parameters guarantee also the isotropy of the acoustic waves. Our objective is to enlarge the domain of validity of our previous study: incorporate the treatment of boundary conditions with rigid walls with a given temperature or adiabatic boundaries, study several couplings between velocity and temperature for elementary Couette and Poiseuille flows, study the possibility of Dirichlet and Neumann boundary conditions. Finally, our objective is the simulation of the de Vahl Davis test case [20] described in Fig. 1.

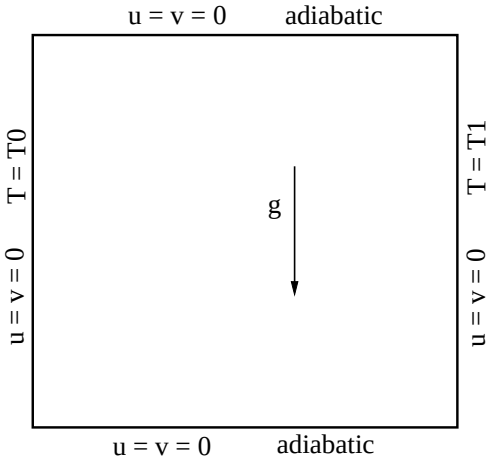


Figure 1: De Vahl Davis test case for natural convection.

https://doi.org/10.4208/cicp.2014.m400 Published online by Cambridge University Press

The outlook of the article is the following. In Section 2, we recall fundamental aspects of the coupled D2Q9-D2Q5 lattice Boltzmann approach. We present our actual choices for the implementation of the lattice Boltzmann approach with the D2Q13 stencil and to treat all the physical fields with single particle distribution and the D2Q13 scheme. In Section 4, we develop a very elementary finite-difference approach for the compressible Navier-Stokes equations. With this tool, we can compare our new D2Q13 approach with a classical reference. In Section 5, we consider a simple test case for non-linear waves. We study the buoyancy in Section 6, the propagation of transverse waves in Section 7, the simulation of Couette flows in Section 8 and Poiseuille flows in Section 9. In Section 10, we consider a test case to take into account various temperature and flux-type boundary conditions. First results for the de Vahl Davis heated cavity are presented in Section 11.

2 Coupled D2Q9-D2Q5 lattice Boltzmann scheme

The Boussinesq approximation of the compressible Navier-Stokes equations can be written as a system of coupled partial differential equations. The unknowns are the vector field of velocity u, and the scalar fields of temperature T and pressure p. The parameters are the shear viscosity ν, the temperature dissipation rate κ, the thermal expansion coefficient β and g the Earth's gravity. The buoyancy term $(1-\beta(T-T_0))g$ is a source term for the momentum equation and the velocity field u directly imposes strong constraints for the transport of temperature. Assuming that the density is $\rho=1$, the equations of the Boussinesq system are

$$\left\{\begin{array}{l} \mathrm{div} u = 0, \\ \dfrac{\partial u}{\partial t} + u\bullet\nabla u + \nabla p - \nu\triangle u = \big(1-\beta(T-T_0)\big)g, \\ \dfrac{\partial T}{\partial t} + u\bullet\nabla T - \kappa\triangle T = 0. \end{array}\right. \tag{2.1}$$

The Rayleigh number is defined from the temperature difference $\Delta T \equiv T_1 - T_0$ between the two sides according to

$$\mathrm{R_a} \equiv \frac{|g|\beta\Delta T L^3}{\nu\kappa}. \tag{2.2}$$

A difficult stationary test case is the computation of the velocity and temperature fields for $\mathrm{R_a} = 10^6$. The references are the original contribution of de Vahl Davis [20], the Le Quéré [15] and the associated workshop in the 2000's with various Navier-Stokes solvers, the introduction of the D2Q9-D2Q5 coupled approximation by Mezrhab *et al.* [16] and the very precise results of Wang *et al.* [21] with the same approach.

Recall that the discrete velocities of a D2Q5 lattice Boltzmann scheme follow the axis of coordinates:

$$v_j \in \{(0,0),(1,0),(0,1),(-1,0),(0,-1)\}, \quad 0 \le j \le 4. \tag{2.3}$$

https://doi.org/10.4208/cicp.2014.m400 Published online by Cambridge University Press

For a D2Q9 scheme we add to the previous D2Q5 velocities (2.3) the four ones along the diagonals:

$$v_j \in \{(1,1),(-1,1),(-1,-1),(1,-1)\}, \quad 5 \leq j \leq 8. \tag{2.4}$$

The flow is simulated with a D2Q9 lattice Boltzmann scheme with 3 conserved moments, the density and the two components of the momentum:

$$\rho \equiv \sum_{j=0}^{8} f_j, \quad (j_x, j_y) \equiv \sum_{j=0}^{8} v_j f_j. \tag{2.5}$$

The six other moments of the fluid are presented in Ref. [11]. The equilibrium values for the moments of order two have to take into account the compressible effects:

$$E^{\rm eq} = \alpha\rho + 3\,\frac{j_x^2+j_y^2}{\rho}, \quad XX^{\rm eq} = \frac{j_x^2-j_y^2}{\rho}, \quad XY^{\rm eq} = \frac{j_x j_y}{\rho}. \tag{2.6}$$

The equilibrium properties either have no influence on the physical properties or are set to give an isotropic shear viscosity. The sound velocity c_s, the shear viscosity μ and the bulk viscosity ζ are given from the previous equilibria according to

$$c_s = \sqrt{\frac{4+\alpha}{6}}, \quad \mu = \frac{1}{3}\Big(\frac{1}{s_{XX}} - \frac{1}{2}\Big), \quad \zeta = -\alpha\Big(\frac{1}{s_E} - \frac{1}{2}\Big). \tag{2.7}$$

The temperature is simulated with a simple D2Q5 scheme with only one conserved moment

$$T \equiv \sum_{j=0}^{4} g_j. \tag{2.8}$$

The other nontrivial equilibrium values follow the relations

$$E^{\rm eq} = \beta\rho, \quad j_x^{\rm eq} = \rho V_x, \quad j_y^{\rm eq} = \rho V_y, \quad XX^{\rm eq} = 0. \tag{2.9}$$

The diffusion coefficient κ is easy to identify:

$$\kappa = \frac{\beta+4}{10}\Big(\frac{1}{s_E} - \frac{1}{2}\Big). \tag{2.10}$$

This D2Q5 model as defined does not satisfy the Galilean invariance with respect to advection at uniform speed $\{V_x, V_y\}$ (see Qian and Zhou [18]); the equivalent equation for the D2Q5 scalar scheme is equal to

$$\frac{\partial T}{\partial t} + V_x\frac{\partial T}{\partial x} + V_y\frac{\partial T}{\partial y} - \kappa\triangle T + \Big(\frac{1}{s_E} - \frac{1}{2}\Big)\Big(V_x^2\frac{\partial^2 T}{\partial x^2} + 2V_xV_y\frac{\partial^2 T}{\partial x\partial y} + V_y^2\frac{\partial^2 T}{\partial y^2}\Big) = 0$$

and can be easily identified with the methods developed *e.g.* in [4].

https://doi.org/10.4208/cicp.2014.m400 Published online by Cambridge University Press

3 Compressible D2Q13 lattice Boltzmann scheme

The stencil of the D2Q13 lattice Boltzmann scheme is built (see *e.g.* [12,13]) on the D2Q9 scheme with the following complementary velocity set:

$$v_j \in \{(2,0),(0,2),(-2,0),(0,-2)\}, \quad 9 \le j \le 12. \tag{3.1}$$

A family of 13 orthogonal moments are generated by an elementary linear mapping of the particle distribution f_j:

$$m_k = \sum_{j=0}^{12} M_{kj} f_j.$$

The coefficients M_{kj} of the matrix are computed from the 13 velocities presented in (2.3), (2.4) and (3.1) with the help of polynomials p_k by the condition

$$M_{kj} = p_k(v_j^x, v_j^y), \qquad 0 \le j,k \le 8. \tag{3.2}$$

The following set $\{p_k\}$ of polynomials are presented in (3.3) as combinations of monomials of increasing power. They have been chosen as symmetric as possible and have been orthogonalized. Instead of giving the final moment matrix, we give the "recipe" to build it in terms of the components $x \equiv v_j^x$ and $y \equiv v_j^y$ of the 13 basic velocities.

$$\left\{\begin{array}{lll}
\text{scalars} & \rho & 1 \\
 & E & -28+13(x^2+y^2) \\
 & \epsilon & 140+(x^2+y^2)(-361/2+77(x^2+y^2)/2) \\
 & \varpi & -12+(x^2+y^2)(\frac{581}{12}+(x^2+y^2)(-\frac{273}{8}+\frac{137}{24}(x^2+y^2))) \\
\text{vectors} & j_x & x \\
 & j_y & y \\
 & q_x & x(3+x^2+y^2) \\
 & q_y & y(3+x^2+y^2) \\
 & r_x & x(\frac{101}{6}+(x^2+y^2)(-\frac{63}{4}+\frac{35}{12}(x^2+y^2))) \\
 & r_y & y(\frac{101}{6}+(x^2+y^2)(-\frac{63}{4}+\frac{35}{12}(x^2+y^2))) \\
\text{tensors} & XX & x^2-y^2 \\
 & XY & x\,y \\
 & XX_e & (x^2-y^2)(-\frac{65}{12}+\frac{17}{12}(x^2+y^2)).
\end{array}\right. \tag{3.3}$$

Following Hénon [7], many formulae can be simplified using

$$\sigma_i \equiv \frac{1}{s_i} - \frac{1}{2}. \tag{3.4}$$

With an asymptotic analysis as the one presented in [13], we can recover the physical waves: two acoustics, one transverse and one longitudinal diffusion. To satisfy correct

https://doi.org/10.4208/cicp.2014.m400 Published online by Cambridge University Press

advection of these four waves in the presence on a uniform background velocity, the following relationships have to be satisfied:

$$\left\{\begin{array}{l} h_1=\dfrac{17}{26}-\dfrac{c_1}{2}-\dfrac{E_0}{13}, \qquad k_1=\dfrac{2}{13}, \\ h_2=-\Big(\dfrac{39}{2}+\dfrac{13}{2}c_1+E_0\Big)\,k_2 \\ \qquad -\dfrac{7}{624}(13\,c_1+95+2\,E_0)\,\dfrac{874481+459459\,c_1-103428\,c_{\epsilon E}+70686\,E_0}{114404+51051\,c_1-11492\,c_{\epsilon E}+7854\,E_0} \end{array}\right. \tag{3.5}$$

for a situation with density equal to 1 and "energy" equal to E_0. In order to enforce isotropy at second order around a null velocity, we have to set

$$\left\{\begin{array}{l} \sigma_{qx}=-\dfrac{1309}{2}\,\dfrac{\sigma_{XX}(13\,c_1+95+2\,E_0)}{114404+51051\,c_1-11492\,c_{\epsilon E}+7854\,E_0}, \\ c_{\epsilon\rho}=140+28\,c_{\epsilon E} \\ \qquad +\dfrac{(13\,c_1+95+2\,E_0)(114404+51051\,c_1-11492\,c_{\epsilon E}+7854\,E_0)}{22984\,Pr}, \\ c_2=-\dfrac{65}{24}-\dfrac{21}{8}(c_1+h_1+k_1\,E_0)-k_2\,E_0-h_2. \end{array}\right. \tag{3.6}$$

These constraints leave as independent parameters: Pr, E_0, c_1, k_2, $c_{\epsilon E}$, $c_{\omega\rho}$, $c_{\omega E}$ and the relaxation rates s_{XX}, s_{rx}, s_ϵ, s_ω and s_{XXe}. The free parameters are chosen to get a stable scheme by computing the roots of the dispersion equation for several values of the wave vector ranging from 0 to 2π in magnitude and several directions with respect to the axis x and y. Our approach is heuristic and nothing *a priori* guaranties the L^2 stability.

4 Navier Stokes solver for a compressible gas

This approach starts from the conservation equations of mass and momentum:

$$\left\{\begin{array}{l} \dfrac{\partial}{\partial t}\rho+\dfrac{\partial}{\partial x}\rho v_x+\dfrac{\partial}{\partial y}\rho v_y=0, \\ \dfrac{\partial}{\partial t}\rho v_x+\dfrac{\partial}{\partial x}\rho v_x v_x+\dfrac{\partial}{\partial y}\rho v_x v_y+\dfrac{\partial}{\partial x}P-\nu\triangle v_x-\zeta\dfrac{\partial}{\partial x}\big(\mathrm{div}\,v\big)=0, \\ \dfrac{\partial}{\partial t}\rho v_y+\dfrac{\partial}{\partial x}\rho v_x v_y+\dfrac{\partial}{\partial y}\rho v_y v_y+\dfrac{\partial}{\partial y}P-\nu\triangle v_y-\zeta\dfrac{\partial}{\partial y}\big(\mathrm{div}\,v\big)=0. \end{array}\right. \tag{4.1}$$

We add also the conservation of total energy. We assume the fluid is a perfect gas, then the pressure P is given according to

$$P=\rho RT \tag{4.2}$$

and the internal energy per unit mass e is related to T by

$$e=\frac{RT}{\gamma-1}. \tag{4.3}$$

https://doi.org/10.4208/cicp.2014.m400 Published online by Cambridge University Press

Then the evolution equation for the internal energy takes the form

$$\left\{\begin{array}{l} \dfrac{\partial}{\partial t}\rho e+\dfrac{\partial}{\partial x}\rho e v_x+\dfrac{\partial}{\partial y}\rho e v_y+P\Big[\dfrac{\partial}{\partial x}u_x+\dfrac{\partial}{\partial y}u_y\Big]-\kappa\Big[\dfrac{\partial^2}{\partial x^2}T+\dfrac{\partial^2}{\partial y^2}T\Big] \\ \qquad -\nu\Big[\Big(\dfrac{\partial}{\partial x}u_x-\dfrac{\partial}{\partial y}u_y\Big)^2+\Big(\dfrac{\partial}{\partial x}u_y+\dfrac{\partial}{\partial y}u_x\Big)^2\Big]-\zeta\Big(\dfrac{\partial}{\partial x}u_x+\dfrac{\partial}{\partial y}v_y\Big)^2=0. \end{array}\right. \tag{4.4}$$

A linearized analysis gives the propagation and damping of the four hydrodynamic modes. We deduce an algebraic expression for the sound velocity c_s, the relaxation ν_τ of the transverse mode, the relaxation $\nu_{\rm diff}$ of the diffusive mode, and the damping $\nu_{\rm acous}$ of the sound modes:

$$c_s=\sqrt{\gamma RT},\quad \nu_\tau=\nu,\quad \nu_{\rm diff}=\kappa\frac{\gamma-1}{R\gamma},\quad \nu_{\rm acous}=\frac{1}{2}(\nu+\zeta)+\frac{(\gamma-1)^2}{2R\gamma}. \tag{4.5}$$

The non-linear terms allow to show that a uniform advection speed $\{V_x,V_y\}$ leads to phase shifts compatible with Galilean invariance.

The model can be approximately simulated with simple finite difference expressions for the space derivatives. We have developed a compressible Navier-Stokes solver for the numerical resolution of the mathematical model (4.1)-(4.4). We use a cell vertex approach (with the nomenclature of Roache [19]). All the differential operators are discretized with centered finite differences. The discrete evolution in times is obtained with an elementary forward Euler first order explicit scheme. The Dirichlet boundary conditions for velocity and temperature are implemented in a clear way by forcing the given value on the boundary node vertex. For the adiabatic wall where $\frac{\partial T}{\partial n}$ is null, a Neumann homogeneous boundary condition is enforced with mirror techniques described in the classical reference [19].

5 A simple test case

This test case has been studied in our contribution [13]. The domain is a $N_x\times N_y$ rectangle with periodic boundary conditions. This test case is error-free as far as boundary conditions are concerned. The initial condition is a fluid at rest: $V_x=V_y=0$. The initial temperature $T(x,y)=T_0+\delta T_0\cos k\bullet x$ is associated with a wave number $k=2\pi K/N_x$. Then density, pressure or energy are such that no acoustic wave is excited. This is possible with the following conditions:

$$\left\{\begin{array}{rl} \text{For D2Q9-D2Q5:} & \rho=1, \\ \text{For D2Q13:} & \rho=1-28\ (T(x,y)-T_0), \\ \text{For Navier Stokes:} & P=RT_0,\ \rho E=\frac{P}{\gamma-1}+\frac{\rho(V_x^2+V_y^2)}{2}. \end{array}\right. \tag{5.1}$$

One verifies that $T(x,y,t)$ relaxes exponentially in time.

https://doi.org/10.4208/cicp.2014.m400 Published online by Cambridge University Press

6 Buoyancy

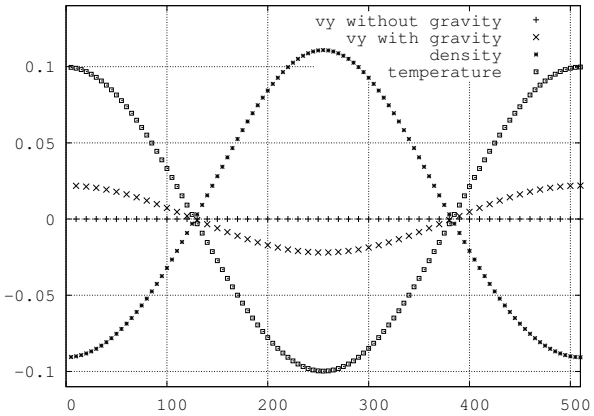


Figure 2: Buoyancy flow with the compressible Navier-Stokes solver. The nonlinear exchanges between temperature and density are not affected by the gravity.

For the first scheme D2Q9-D2Q5 we simulate buoyancy by adding a vertical force (V_y) proportional to $T-T_0$. For the D2Q13 scheme and the direct approach of Navier-Stokes equations with finite differences, we add vertical force in the V_y momentum equation proportional to $\rho-\rho_0$. Then the vertical speed increases approximately linearly with time and there is essentially no horizontal velocity. With the Navier-Stokes solver, we use a domain composed by 510 mesh points in width, and periodic in height. The temperature is periodic relative to the x direction. With the D2Q13 lattice Boltzmann solver, we use the same domain as previously: a domain of 510 meshes in width and periodic in height, with an (initial) temperature periodic in x (see Fig. 3).

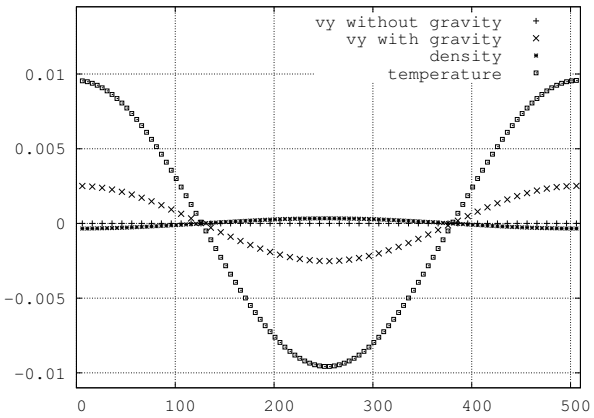


Figure 3: Buoyancy flow with the D2Q13 direct lattice Boltzmann solver. The nonlinear exchanges between temperature and density are not affected by the gravity.

https://doi.org/10.4208/cicp.2014.m400 Published online by Cambridge University Press

7 Transverse waves

With the D2Q13 stencil, the non linear behaviour for transverse waves is operating as follows. The initial conditions $v_y(x,y,0)\equiv V_{y0}\cos kx$ leads to density waves of wave vector $2k$. We modify the initial conditions by $\rho(x,y,0)=\rho_0+a\ v_y(x,y,0)^2$. We measure the following global aggregates relative to time:

$$\tilde{V}_y(t)=\sum_x v_y\cos(k\,x),\quad \tilde{\rho}(t)=\sum_x \rho\cos(2\,k\,x),\quad \tilde{E}(t)=\sum_x E\cos(2\,k\,x). \tag{7.1}$$

The typical result for D2Q13 is summarized in Fig. 4: the growth of $\tilde{E}$ in time is proportional to $\nu k^2 V_y^2$.

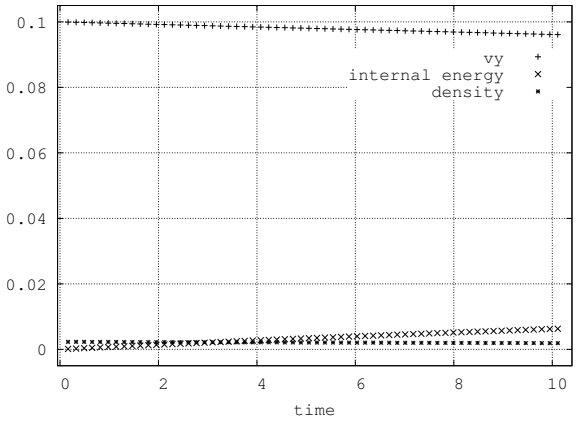


Figure 4: Boltzmann solver. The growth of $\tilde{E}$ in time is proportional to $\nu k^2 V_y^2$.

The interpretation of this evolution can be stated as follows. The linearized equivalent equations at order 1 with space derivatives can be written in matrix form

$$\begin{vmatrix} \partial_t & \partial_r & 0 \\ (\frac{14}{13}+\frac{1}{2}V^2)\,\partial_r & \partial_t & \frac{1}{26}\partial_r \\ 0 & \frac{1}{2}(39+13c_1+2E_0)\,\partial_r & \partial_t \end{vmatrix}=0. \tag{7.2}$$

Without advective velocity, the diffusive mode is $(1,0,-28)^{\mathsf{t}}$ *id est* $E=-28\rho$. With a transverse velocity V, the diffusive mode is equal to $(1,0,-28-13V^2)^{\mathsf{t}}$, *id est* $E=-28\tilde{\rho}$ with a density ρ replaced by $\tilde{\rho}\equiv 1+\frac{13}{28}V^2$.

8 Couette flows

Typical boundary conditions for Couette flows with the D2Q9-D2Q5 scheme are stated as follows. For $x=1$ and $x=N_x$ the velocity is known: $V_x=0$ and V_y is given. This type

https://doi.org/10.4208/cicp.2014.m400 Published online by Cambridge University Press

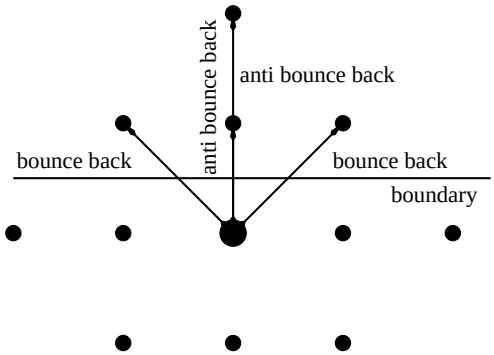


Figure 5: Mixed "bounce-back" and "anti-bounce-back" boundary conditions for a flow simulated with the D2Q13 lattice Boltzmann scheme. In this case, both velocity and temperature are imposed.

of boundary condition is classically achieved by a "bounce-back" condition. Assuming a zero value for the mean temperature, for $x=1$ the temperature is imposed: $T=+\Delta T$ and when $x=N_x$ it has the opposite sign: $T=-\Delta T$ for $x=N_x$. This boundary condition is achieved by an "anti-bounce-back" as proposed by Ginzburg [6]. In consequence, the way we implement the boundary conditions is not straightforward. For the unit velocities with non-zero component parallel to the boundary, we use a bounce-back boundary condition. For the other velocities, an "anti-bounce-back" is implemented. We consider for example:

$$f_1+f_3=2\,(p_\rho\,\rho+p_{XX}\,XX+p_E\,E) \tag{8.1}$$

with E and XX imposed and ρ estimated by extrapolation from values measured in the fluid.

With the coupled D2Q9-D2Q5 scheme, the density is unchanged (see Fig. 6). For the discretization of the compressible Navier Stokes equations, the pressure remains con-

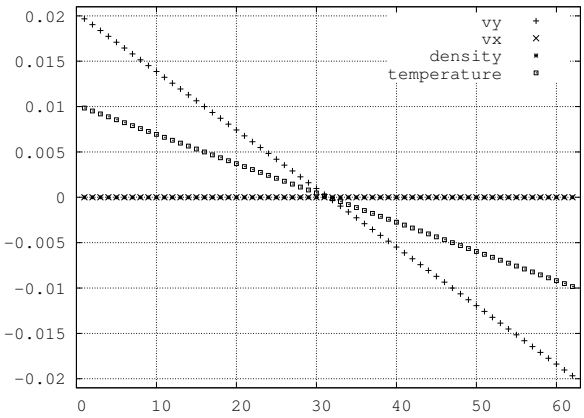


Figure 6: Couette flow with the D2Q9-D2Q5 coupled scheme. Result for the temperature field without motion of the lateral plates.

https://doi.org/10.4208/cicp.2014.m400 Published online by Cambridge University Press

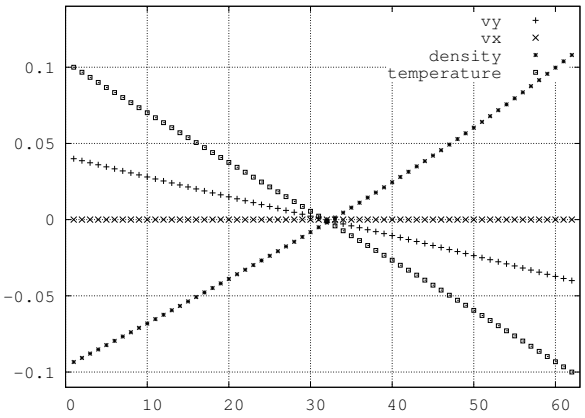


Figure 7: Couette flow with a finite difference direct Navier-Stokes solver. Same result for the temperature field without motion of the plates.

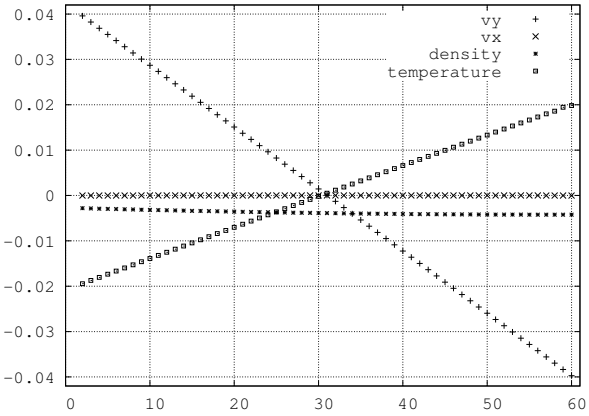


Figure 8: Couette flow with the D2Q13 lattice Boltzmann solver. The dashed curves show the "temperature" $T \equiv E - \frac{13}{2}(V_x^2 + V_y^2)$. There is no variation of the temperature when no gradient is imposed between the plates.

stant. Then, due to the equation of state (4.2), the variation of density and temperature are coupled. This effect is clearly visible in the Fig. 7 (direct Navier Stokes solver) With the D2Q13 lattice Boltzmann scheme, the internal energy e (proportional to the temperature) can be recovered thanks to the relation $e = E - \frac{13}{2}(V_x^2 + V_y^2)$ as displayed in Fig. 8.

9 Poiseuille flow

A Poiseuille flow is realized by adding an external term to take into account the gradient of pressure. Then a parabolic velocity profile is obtained as usual. Moreover, we add a Couette-type temperature profile between the lateral plates. In all our simulations, we

https://doi.org/10.4208/cicp.2014.m400 Published online by Cambridge University Press

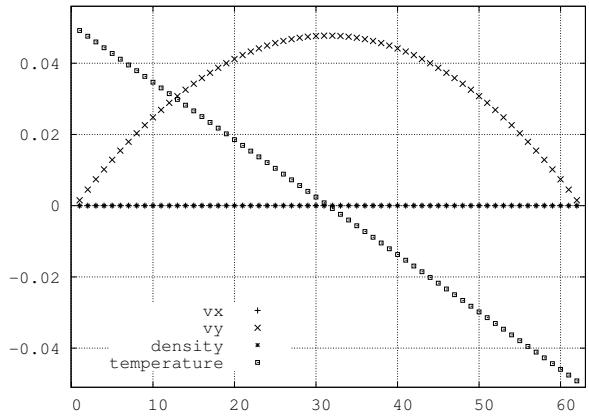


Figure 9: Poiseuille flow with the D2Q9-D2Q5 coupled scheme. No variation of the temperature when no gradient is imposed between the plates.

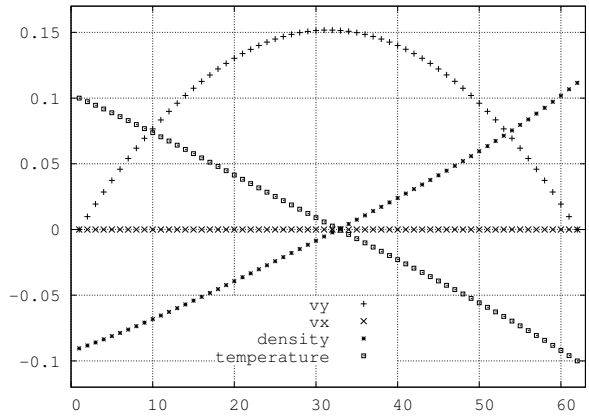


Figure 10: Poiseuille flow with a finite difference direct Navier-Stokes solver. No variation of the temperature when no gradient is imposed between the plates.

do not observe any variation of the temperature when no gradient is imposed between the plates. Moreover, when a gradient of temperature is imposed, we observe a regular evolution of the temperature without destruction of the parabolic profile.

10 Test of an adiabatic boundary for the D2Q13 scheme

In order to implement correctly a null flux Neumann boundary condition relative to the temperature, we have tested our schemes for a uniform volumic source of energy. A homogeneous temperature given at the left boundary and a homogeneous Neumann condition for temperature at the right boundary. At the left boundary the velocity is given as homogeneous or inhomogeneous: $v_y = 0$ or $v_y = 0.02$. We impose a null velocity

https://doi.org/10.4208/cicp.2014.m400 Published online by Cambridge University Press

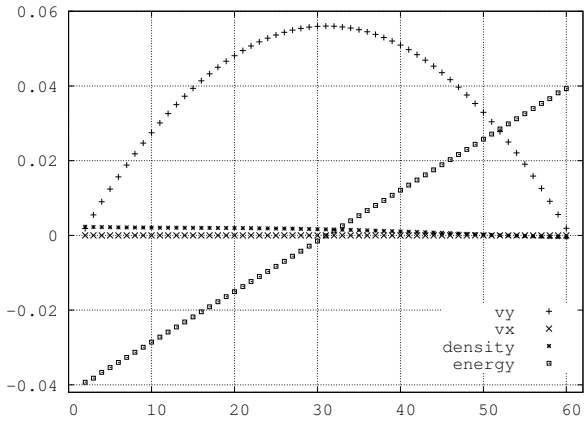


Figure 11: Poiseuille flow with the D2Q13 lattice Boltzmann scheme. No variation of the temperature when no gradient is imposed between the plates.

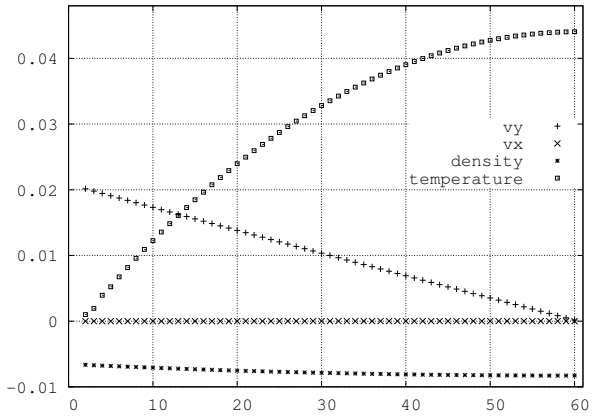


Figure 12: Test of an adiabatic boundary with the D2Q13 lattice Boltzmann solver. A uniform source of energy is applied. The y-velocity is null when the left boundary is fixed. The other fields are unchanged.

at the right boundary. The solution is a "semi-parabol" and is correctly simulated as described in Fig. 12.

11 Thermal test case of de Vahl Davis

The de Vahl Davis [20] test has been described in the introduction. We have used a 187×187 domain with a Prandtl number equal to 0.71 with the lattice Boltzmann simulations and a grid with 256×256 mesh points. For the simple Navier-Stokes solver with finite differences, we have used 128×128, 196×196 and 256×256 mesh sizes. The results for the mean Nusselt number is respectively equal to 4.5099, 4.5154 and 4.5157 for a Rayleigh number equal to 10^5. Our results are globally summarized in the following

https://doi.org/10.4208/cicp.2014.m400 Published online by Cambridge University Press

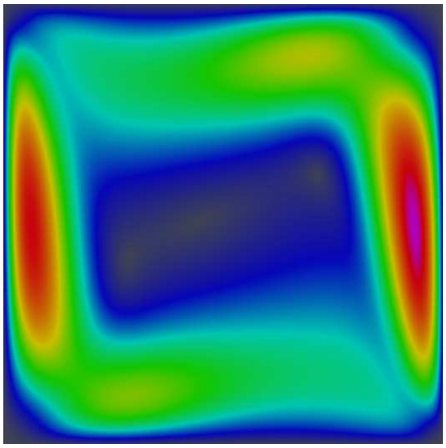


Figure 13: De Vahl Davis thermal test case for natural convection with the D2Q13 direct lattice Boltzmann solver. Rayleigh number $= 10^5$. Iso-velocity curves for the modulus of the fluid speed. The maximum velocity is 5.5 10^{-3}.

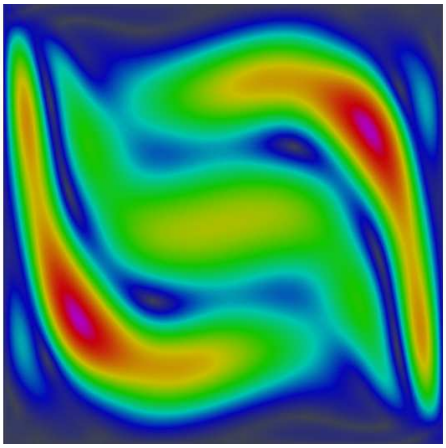


Figure 14: De Vahl Davis thermal test case for natural convection with the D2Q13 direct lattice Boltzmann solver. Rayleigh number $= 10^5$. Modulus of the asymmetry of the fluid speed. Curves for the departure from center symmetry. The maximum difference of velocity $|V(x,y)+V(x_0-x,y_0-y)|$ is 0.28 10^{-3} (5 %).

table. Simulations have been done on graphics card and implemented with Cuda. We do not have precise comparisons of execution times between the two lattice Boltzmann models. We estimate the overhead to be roughly +20 % for D2Q13 compared to the coupled D2Q9-D2Q5.

We have compared our results with those of de Vahl Davis [20], Le Quéré [15], Mezhrab *et al.* [16], Wang *et al.* [21] with the coupled approach D2Q9-D2Q5 and our simple finite differences Navier-Stokes solver. The results "D2Q13" obtained with a single particle distribution are correct but must be considered as preliminary compared to the other results. Inspection of the thermal and velocity fields obtained with the D2Q9-D2Q5 shows

https://doi.org/10.4208/cicp.2014.m400 Published online by Cambridge University Press

Table 1: Comparison of Nusselt number integrated in the whole cavity for two Rayleigh numbers.

Rayleigh	de Vahl Davis	Le Quéré	Mezrhab	D2Q9-D2Q5	Navier Stokes	D2Q13
10^5	4.519		4.521	4.521	4.51	4.50
10^6	8.800	8.8252	8.824	8.828	8.88	8.73

that they are symmetric with respect to the center of the cavity. Similar inspection for the fields obtained either with D2Q13 or the simple compressible Navier-Stokes code used here show disymmetries that increase with the Rayleigh number. A detailed analysis of these asymmetries will be performed later and checked with data obtained with more sophisticated Navier-Stokes codes.

12 Conclusion

In this contribution, we have shown that coupled fluid and thermal flows that characterize natural convection can be simulated in two space dimensions with a single D2Q13 lattice Boltzmann scheme by imposing the conservation of mass, momentum and energy. We have tested our approach by a progressive complexification of the test cases. Observe that strong compressible effects including the simulation of shock waves have not been considered in this contribution. The de Vahl Davis test case for natural convection gives encouraging results when we compare our result to previous ones obtained with a D2Q9-D2Q5 coupled approach or with a direct simulation of the compressible Navier Stokes equations with finite differences. Our results show that a lattice Boltzmann model with a single D2Q13 distribution that conserves mass, momentum and energy gives results that compare better to direct Navier-Stokes simulations with finite differences than with simulations obtained with the Boussinesq approximation. Nevertheless, complementary studies are necessary to improve this method of simulation and confirm our results.

Acknowledgments

The authors thank the two anonymous referees for their very constructive remarks. Many thanks also to the "LaBS project" (Lattice Boltzmann Solver, www.labs-project.org), funded by the French FUI8 research program, for supporting this contribution.

References

[1] G.K. Batchelor. An Introduction to Fluid Dynamics, Cambridge University Press, 1967.
[2] R. Benzi, S. Succi, Vergassola "The lattice Boltzmann equation: theory and applications", Physics Reports, vol. 222, pp. 145-197, 1992.

https://doi.org/10.4208/cicp.2014.m400 Published online by Cambridge University Press

[3] F. Dubois. "Stable lattice Boltzmann schemes with a dual entropy approach for monodimensional nonlinear waves", Computers and Mathematics with Applications, vol. 65, pp. 142-159, 2013.
[4] F. Dubois, P. Lallemand. "Towards higher order lattice Boltzmann schemes", Journal of Statistical Mechanics: Theory and Experiment, P06006, 2009.
[5] J. Eggels, J. Somers. "Numerical-simulation of free convective flow using the lattice-Boltzmann scheme", International Journal of Heat and Fluid Flow, vol. 16, pp. 357-364, 1995.
[6] I. Ginzburg. "Generic boundary conditions for lattice Boltzmann models and their application to advection and anisotropic dispersion equations", Advances in Water Resources, vol. 28, pp. 1196-1216, 2005.
[7] M. Hénon. "Viscosity of a Lattice Gas", Complex Systems, vol. 1, pp. 763-789, 1987.
[8] D. d'Humières. "Generalized Lattice-Boltzmann Equations", in Rarefied Gas Dynamics: Theory and Simulations (Eds B.D. Shizgal and D.P. Weave), vol. 159 of AIAA Progress in Astronautics and Astronautics, pp. 450-458, 1992.
[9] M. Junk, A. Klar, L.S. Luo. "Asymptotic analysis of the lattice Boltzmann equation", Journal of Computational Physics, vol. 210, pp. 676-704, 2005.
[10] B. Khobalatte, B. Perthame. "Maximum principle on the entropy and second-order kinetic schemes", Mathematics of Computation, vol. 62, pp. 119-131, 1994.
[11] P. Lallemand, L.-S. Luo. "Theory of the lattice Boltzmann method: Dispersion, dissipation, isotropy, Galilean invariance, and stability", Physical Review E, vol. 61, pp. 6546-6562, June 2000.
[12] P. Lallemand, L.-S. Luo. "Theory of the lattice Boltzmann method: Acoustic and thermal properties in two and three dimensions", Physical Review E, vol. 68, pp. 036706, 2003. vol. 68, no. 3, 2003
[13] P. Lallemand, F. Dubois. "Some results on energy-conserving lattice Boltzmann models", Computers and Mathematics with Applications, vol. 65, pp. 831-844, 2013.
[14] L.D. Landau, E.M. Lifshitz. Fluid Mechanics, Pergamon Press, 1959.
[15] P. Le Quéré. "Accurate solutions to the square thermally driven cavity at high Rayleigh number", Computers and Fluids, vol. 20, pp. 29-41, 1991.
[16] A. Mezrhab, A. Moussaoui, M. Jami, H. Naji. "Double MRT thermal lattice Boltzmann method for simulating convective flows", Physics Letters A vol. 374, pp. 3499-3507, 2010.
[17] X. Nie, X. Shan, H. Chen. "Thermal lattice Boltzmann model for gases with internal degrees of freedom", Physical Review E, vol. 77, pp. 035701(R), 2008.
[18] Y. Qian, Y. Zhou. "Complete Galilean-invariant lattice BGK models for the Navier-Stokes equation", Europhysics Letters, vol. 42, pp. 359-364, 1998.
[19] P.J. Roache. Computational Fluid Dynamics, 446 pages, Hermosa Publishers, Albuquerque, 1976.
[20] G. De Vahl Davis. "Natural convection of air in a square cavity: A benchmark numerical solution", Int. J. of Num. Meth. in fluids, vol. 3, pp. 249-264, 1983.
[21] J. Wang, D. Wang, P. Lallemand, L-S. Luo. "Lattice Boltzmann simulations of thermal convective flows in two dimensions", Computers and Mathematics with Applications, vol. 65, pp. 262-286, 2013.

https://doi.org/10.4208/cicp.2014.m400 Published online by Cambridge University Press